HHS Public Access

Author manuscript

Neuron. Author manuscript; available in PMC 2017 June 15.

Published in final edited form as:

Neuron. 2016 June 15; 90(6): 1174–1188. doi:10.1016/j.neuron.2016.05.005.

A Primate lncRNA Mediates Notch Signaling During Neuronal Development by Sequestering miRNA

Neha Rani[1], **Tomasz J Nowakowski**[2,3], **Hongjun Zhou**[1], **Sirie E. Godshalk**[1], **Véronique Lisi**[1], **Arnold R. Kriegstein**[2,3], and **Kenneth S. Kosik**[1]

[1]Neuroscience Research Institute and Department Molecular, Cellular and Developmental Biology, University of California, Santa Barbara, Santa Barbara, CA 93106, USA

[2]Eli and Edythe Broad Center of Regeneration Medicine and Stem Cell Research, University of California, San Francisco, San Francisco, CA 94143, USA

[3]Department of Neurology, University of California, San Francisco, San Francisco, CA 94158, USA

Summary

Long non-coding RNAs (lncRNAs) are a diverse and poorly conserved category of transcripts that have expanded greatly in primates, particularly in the brain. We identified a lncRNA, which has acquired 16 microRNA response elements for miR-143-3p in the Catarrhini branch of primates. This lncRNA termed *LncND* (neuro-development) is expressed in neural progenitor cells and then declines in neurons. Binding and release of miR-143-3p, by *LncND*, controls the expression of Notch receptors. *LncND* expression is enriched in radial glia cells (RGCs) in the ventricular and subventricular zones of developing human brain. Down-regulation in neuroblastoma cells reduced cell proliferation and induced neuronal differentiation, an effect phenocopied by miR-143-3p over-expression. Gain-of-function of *LncND* in developing mouse cortex led to an expansion of PAX6+ RGCs. These findings support role for *LncND* in miRNA-mediated regulation of Notch signaling within the neural progenitor pool in primates that may have contributed to the expansion of cerebral cortex.

Introduction

Long non-coding RNAs (lncRNAs) have complex and diverse functions in brain development. lncRNAs have relatively low levels of evolutionary conservation with

Correspondence: kosik@lifesci.ucsb.edu (K.S.K.).

Author Contributions

K.S.K. and N.R. conceived and supervised the project. N.R. designed and performed the experiments. Bioinformatic analysis was performed by H.Z., V.L. and N.R. Cerebral organoids generation and single-cell sequencing was performed by S.E.G. *in-utero* electroporation experiment was performed by T.J.N. in the lab of A.R.K. Manuscript was prepared by N.R. and K.S.K. with critical suggestions from T.J.N.

The authors declare no competing financial interests.

sequence deletions, insertions (Mclean et al., 2003) and accelerated nucleotide substitution (Pollard et al., 2006) at evolutionary divergences. About a third of the lncRNAs are unique to the primate lineage (Derrien et al., 2012), and only ~12% of human lncRNAs appear to be conserved in other vertebrate species (Ulitsky and Bartel, 2013; Cabili et al., 2011). The restricted spatial and temporal expression patterns of many lncRNAs within the brain likely contributes to neuronal diversification in large brain primates (Amaral and Mattick, 2008; Cao et al., 2006; Chodroff et al., 2010; Qureshi et al., 2010) and the specification of individual neuronal subtypes (Mercer et al., 2008).

MicroRNAs (miRNAs) are derived from hairpin precursors that function in association with Argonaute proteins to regulate target genes post-transcriptionally. These ~ 21–23 nucleotide sequences change quite dramatically as cells transition from germ cells to neural stem cells and at all stages of cell differentiation during brain development (reviewed in Fineberg et al., 2009). The many regulatory controls over miRNA levels and cell type specific expression, include the well-known panoply of gene expression mechanisms, e.g. promoters, enhancers and epigenetic modifications; as well as degradation and biogenesis pathways (Ha and Kim, 2014).

An additional source of control over the levels of mature miRNAs is their sequestration and release from binding sites, known as miRNA response elements (MREs) in transcribed pseudogenes, long non-coding RNAs (lncRNAs) and circular RNAs (Cesana et al., 2011; Ebert and Sharp, 2010; Hansen et al., 2013; Kallen et al., 2013; Memczak et al., 2013; Tay et al., 2011, 2014; Wang et al., 2013; Zhang et al., 2013). These natural miRNA-binding platforms known as sponges contain MREs that can relieve mRNA targets from repression or indirectly induce target mRNA repression by release of miRNAs from this reservoir. Natural miRNA sponges impart stability to miRNAs (Bail et al., 2010) by sequence-specifically sequestering miRNAs directed toward specific mRNA targets within Argonaute protein complexes. Short stretches of complementarity to miRNA seeds in regions of relatively unstructured RNA found in lncRNAs could evolve easily (Ebert and Sharp, 2010).

lncRNAs have the potential to sponge miRNAs, and thereby, regulate the expression of mRNAs (Hu et al., 2012; Wang et al., 2013; Wang et al., 2010; Kallen et al., 2013; Tay et al., 2014; Cesana et al., 2011). The first of these was discovered in plants (Franco-Zorrilla et al., 2007) and others have been described during muscle development (Legnini et al., 2014; Cesana et al., 2011; Kallen et al., 2013), and in embryonic stem cells to regulate core pluripotency transcription factors (Wang et al., 2013). The *H19* lncRNA has been detected in a complex with miR-17-5p by photo-crosslinking and Argonaute 2 immunopurification (Imig et al., 2014).

We identified and functionally characterized a lncRNA, *LncND* (lncRNA for Neuronal Development) that is deleted in a region of the genome associated with a human neurodevelopmental disorder. A microdeletion at 2p25.3 includes *LncND* and 6–7 protein-coding genes (Stevens et al., 2011; Rio et al., 2013; Doco-Fenzy et al., 2014; Bonaglia et al., 2014). Six individuals harboring 2p25.3 terminal or interstitial deletions of different sizes, all including *LncND,* had intellectual disability (Stevens et al., 2011). A set of monozygotic twins with a karyotype involving this genomic locus had a discordant phenotype: one with a

heterozygous deletion of the 2p25.3 region exhibited developmental delay, absence of speech, hyperactivity and the other harbored somatic mosaicism had autism spectrum disorder (Rio et al., 2013). Five patients with a deletion of the subtelomeric region of chromosome 2 (size 2.90–2.97 Mb) had intellectual disability with aggressive outbursts and hyperactivity (Doco-Fenzy et al., 2014). The deleted region included Ysc84-like-1 (*SH3YL1*), acid phosphatase 1 soluble (*ACP1*), trans-membrane protein 18 (*TMEM18*), syntrophin gamma 2 (*SNTG2*), thyroid peroxidase (*TPO*), Drosophila peroxidasin homologue (*PXDN*), myelin transcription factor 1-like (*MYT1L*) (Figure S1a), and uncharacterized long-non coding RNAs, including *LncND*. We demonstrated that *LncND* acts as a miRNA sponge for miR-143-3p and in so doing can regulate the Notch signaling pathway. The knock-down of *LncND* in neuroblastoma cells repressed NOTCH-1 and NOTCH-2 and differentiated the cells to neurons. RNA-seq analysis indicated a significant number of differentially expressed overlapping genes (including cell-cycle related and neurogenesis genes) after *LncND* knock-down or miR-143-3p over-expression. Single-cell analysis and *in-situ* hybridization confirmed the high expression of *LncND* in radial glia cells in human cortex suggesting its role in maintaining the neural progenitor pool during the expansion of the cerebral cortex by regulating the Notch signaling pathway. This conclusion was supported by a functional assay in which expansion of the radial glial population occurred following *in vivo* overexpression of *LncND*.

RESULTS

Characterization of lncRNA with Multiple miRNA Response Elements

Recently, a reference catalog of more than 8000 human lncRNAs was defined from about four billion RNA-seq reads across 24 tissues and cell types (Cabili et al., 2011). A stringent set of 4662 high quality human lncRNA loci (14,353 transcripts) was annotated (Human Body Map LincRNAs, Broad Institute). We focused on brain expressed lncRNAs and selected 358 lncRNA loci (1175 transcripts) that were expressed (fpkm >=1) in two biological replicates from the database. TargetScan (Lewis et al., 2005) was used to predict miRNA binding sites along these full-length lncRNAs. 53 brain expressed miRNAs were selected from profiling 40 normal human tissues (Liang et al., 2007). We postulated that the tendency of an RNA to act as a miRNA sponge will increase with an increasing number of miRNA Response Elements (MREs). Taking these factors into consideration, we identified four lncRNA loci (6 transcripts) with 10 or more MREs for a single miRNA (Figure 1A).

The transcript, TCONS_00003534 transcript (sense strand), has multiple MREs for several miRNAs spread over a relatively short sequence segment. However, with further computational analysis, we observed contradictory information on the directionality of this transcript. RNA-sequencing data from hiPSC-derived neurons (M.A. Lalli., I. Hernandez, and K.S.K., unpublished data) and RNAseq data on the UCSC Genome Browser showed most of the reads derived from the antisense strand, contrary to the annotation in the Human Body Map LincRNAs catalog. The antisense transcript, hereafter referred to as lncRNA for Neuronal Development or *LncND*, is located on chromosome 2: 663814–666523 (2p25.3 arm of chromosome 2) with seven protein-coding genes in its vicinity (Figure S1A). Several marks of active transcription and conserved regulatory elements are present upstream of the

LncND locus (http://genome.ucsc.edu/) (Kent et al., 2002) (Figure S1B). There were multiple MREs for several miRNAs on the antisense strand, among them, miR-143-3p, miR-4286, miR-1912 and miR-4330 (Figure 1B).

To confirm the strand usage of this lncRNA, we performed *in situ* hybridization (ISH) on undifferentiated human embryonic stem cells (H9 cells) before and after differentiation into neural progenitor cells (NPCs) by dual SMAD inhibition (SMADi) (Chambers et al., 2009). Consistent with our RNAseq data from the hiPSC-derived neurons, only the antisense strand was expressed in NPCs (Figure 1C, top). No signal was detected in undifferentiated H9 cells (Figure S1C). We obtained the same result with the antisense probe in human neuroblastoma cell line, SHSY5Y (Figure 1C, bottom). The signal was localized in the nucleus and the cytoplasm (Figure 1C, black arrows-cytoplasmic and red arrows-nuclear). Therefore, a mis-annotation of the strand usage is present in the Human Body Map LincRNAs catalog, likely due to the use of a sequencing method which lacked strand specificity (Cabili et al., 2011).

Cabili et al., predicted four splice variants of *LncND*. One of these isoforms (TCONS_00003534) was identified with a small intron (59 bases from 758–816 bp) between two exons (1–757 bp and 817–2651 bp) with a full transcript of 2651 bp. Fragments of the full-length *LncND* transcript with overlapping regions were successfully amplified from human brain RNA (FirstChoice Human Brain Total RNA from Ambion) using either random hexamers (Figure S1D) or oligo-dT primers (Figure S1E). Therefore, the predicted intron sequence (between 758–816 bp) is part of an exon suggesting that the transcript might be expressed as a single large exon similar to MALAT1 and NEAT1 lncRNAs (Hutchinson et al., 2007; Ji et al., 2003).

LncND is poorly conserved with a primate specific insertion in the 5′ end of *LncND* RNA (Multiz Alignment, Figure 1D). Interestingly, most of the MREs are located in the primate-specific region (Figure 1D, 1B). The phylogeny tree, created by phylogeny.fr (Dereeper et al., 2008), shows that the *LncND* sequences among Catarrhini (Old World Monkeys including, Rhesus, Green Monkey, Baboon and Crab-eating Macaque, and Apes including, Chimpanzee, Gorilla, Orangutan and Gibbon and Humans) are closely related, and the MREs for miR-143-3p are less conserved in Platyrrhini (New World Monkeys including, Squirrel monkeys and Marmoset) compared to Catarrhini (Figure 1E).

Expression of *LncND* During Neuronal Differentiation

To determine the expression of *LncND* during development, we differentiated H9 hESCs either into neurons through intermediate stages using dual SMAD inhibitors (Chambers et al., 2009) or into mesendoderm using BMP4 and FGF2 (Yu et al., 2011). SMAD inhibition directed the stem cells specifically towards neuroectoderm in which mRNA expression of *PAX6*, *SOX2*, *NES* and *HES1*, were highly up-regulated at day five of differentiation (Figure S2A, B). Markers for endoderm (*GATA6*) and mesoderm (*Brachyury* or the *T* gene) were low (C_t values lower than 30) (Figure. S2A). With further differentiation to neurons, *PAX6* was down-regulated (Figure S2A) and immuno-staining with Tau- and MAP2-specific antibodies became apparent (Figure S2C). *LncND* expression increased in neural progenitors at day 5 of differentiation and then dropped rapidly in neurons (Figure 2A). We also measured the expression of *LncND* using a second model of neuronal differentiation

(passage through embryoid bodies and neurospheres) and again observed a gradual increase in the expression of *LncND* till the neurosphere stage, followed by a decrease in its expression in neurons (data not shown). When H9 cells were differentiated into mesendoderm, *GATA6* and *Brachyury* mRNA were highly up-regulated at day 5 (Figure S2D). *PAX6* was expressed at very low levels in these cells, consistent with differentiation towards mesendoderm (Figure S2D). *LncND* expression remained stable at day 2 and down-regulated at day 5 of mesendoderm differentiation (Figure 2B). The expression of *LncND* in SHSY5Y cells exceeded the levels of neural stem cells at day 5 of differentiation of H9 cells (Figure S2E). Thus, *LncND* is preferentially elevated in early neural progenitor cells, suggesting its selective role during neuronal differentiation.

miR-143-3p Binds to *LncND*

Near-perfect complementarity at the "seed region" from position 2–7 at the 5′end of the miRNA determines target specificity (Friedman et al., 2009; Ellwanger et al., 2011; Betel et al., 2010). PITA algorithm (Kertesz et al., 2007) predicted 16 putative MREs for miR-143-3p at the 5′end of the *LncND* (Figure 1B). All these sites, except one with a 7mer-1A site, are perfect 6-mer sites together with complementarity at the 3′ end of miRNA (Lewis et al., 2005; Bartel, 2009). A large number of MREs for several other miRNAs were found including miR-4286, miR-1912 and miR-4330 (Figures 2C and 1B). A thermodynamic energy prediction between *LncND* and miR-143-3p sites indicated highly negative ΔG values for all of its sites (Figure 2D). The other three potential miRNAs also had very low ΔG values (Figure S3).

A miRNA sponge is expected to form a complex with Ago2, a component of the RNA-induced silencing complex (RISC) (Gregory et al., 2005; Meister et al., 2004). *LncND* was highly enriched (~ 6–7 fold) in Ago2 immunoprecipitation with an Ago2-specific antibody in SHSY5Y cells as compared to the IgG control (Figure 2E, 2F). As a positive control, we observed ~8–9 fold enrichment of *H19* lncRNA in Ago2-IP (Figure 2F), which was previously identified as a miRNA sponge enriched in an Ago2-IP (Kallen et al., 2013). *GAPDH*, used as a negative control, was only ~ 2 fold enriched (Figure 2F). This finding suggests that *LncND* is associated with the RISC in a setting where it might compete for the binding of miRNAs "shared" with target mRNAs.

To verify a direct interaction between miR-143-3p and *LncND*, the 5′ end of *LncND* (1–1511 bp) was cloned in pMIR-Report vector and the luciferase reporter assay was performed in HEK293T cells. When luciferase fused to *LncND* was expressed in the presence of the miR-143-3p mimic, the luciferase signal was reduced. This finding suggested that miR-143-3p can bind to the 5′ end of *LncND* with functional consequences (Figure 2G). The LNA-inhibitor for miR-143-3p caused a substantial increase in the luciferase activity of *LncND* in SHSY5Y cells. (Due to negligible expression of miR-143-3p in HEK293T cells, we used SHYS5Y cells for LNA-inhibition) (Figure 2H). Interestingly, the miR-143-3p mimic did not destroy the endogenous *LncND* RNA in SHSY5Y cells, suggesting high stability of the *LncND*-miR-143-3p complex, which is an expected property of a miRNA sponge (Figure 2I). As observed by luciferase activity assay, miR-4330 could also bind to *LncND* (data not shown), but not miR-4286, nor miR-1912, suggesting that at least two

miRNAs could be targeted by *LncND*. These results suggested that *LncND* could potentially serve as a miRNA sponge as it binds to miR-143-3p, but is not degraded by the miRNA.

miR-143-3p Targets Notch

High *LncND* expression in neural progenitors but not in neurons, suggested that *LncND* could regulate an early neuronal differentiation pathway. Among neurodevelopmental genes *NOTCH-1* and *NOTCH-2* 3′UTR had one MRE for miR-143-3p (Figure 3A). The Notch signaling pathway is involved in differentiation, development, proliferation, cell fate decision, and survival in brain (Shimojo et al., 2008; Artavanis-Tsakonas, 1999; Gaiano and Fishell, 2002; Fox et al., 2008; Louvi and Artavanis-Tsakonas, 2006). miRNA binding sites of the top four miRNAs on the 3′UTR of *NOTCH-1* and *NOTCH-2* are represented in the table (Figure 2C). To confirm the predicted binding of miR-143-3p to the 3′UTR of *NOTCH-1* and *NOTCH-2*, we transiently expressed miR-143-3p mimic in HEK293T cells or the LNA inhibitor of miR-143-3p in SHSY5Y cells together with the luciferase reporter plasmids for either *NOTCH-1* or *NOTCH-2* 3′UTR. The reduction or increase in the luciferase activity in the presence of miRNA mimic or LNA inhibitor confirmed the potential binding sites for miR-143-3p in the 3′UTR of *NOTCH-1* and *NOTCH-2* in HEK293T cells (Figure 3B, 3C).

Furthermore, the expression of endogenous *NOTCH-1* and *NOTCH-2* mRNA and protein were significantly down-regulated in the presence of the miR-143-3p mimic (Figure 3D, F). The downstream targets of Notch signaling pathway, *HES1* and *HEY1* were also down-regulated (Figure 3E), confirming the effect on this pathway by miR-143-3p. Moreover, inhibition of miR-143-3p in SHSY5Y cells, up-regulated the expression of endogenous NOTCH-1 and NOTCH-2 protein (Figure 3G). These results support *NOTCH-1* and *NOTCH-2* mRNA as miR-143-3p targets, for which *LncND* may serve as a reservoir. miR-4330 can also down-regulate *NOTCH-1* and *NOTCH-2* (data not shown); however we did not pursue this further because the expression of this miRNA was very low during the differentiation of stem cells.

Interestingly, like *LncND*, the miR-143-3p MRE region of NOTCH has undergone active evolutionary change, albeit over a longer time interval than *LncND. NOTCH-2* lacks the miR-143-3p MRE in rodents and ferrets; however the MRE is conserved in *NOTCH-1* (Figure S4).

LncND Sequesters miR-143-3p to Regulate Notch

Assuming that *LncND* can compete with the 3′UTR of *NOTCH-1* or *NOTCH-2* for the binding of miR-143-3p, we would expect that luciferase fused to the 3′ UTR of either *NOTCH-1* or *NOTCH-2* would show increased activity when *LncND* is over-expressed. The overexpression or knock-down of *LncND*, in SHSY5Y cells, in the presence of the 3′UTR of *NOTCH-1* and *NOTCH-2* fused to luciferase, resulted in up-regulation or down-regulation respectively of the luciferase activity (Figure 4A, 4B). These results suggest that *LncND* sequesters miR-143-3p to regulate NOTCH-1 and NOTCH-2 expression.

Upon the knock-down of *LncND* in SHSY5Y cells (~50% knock-down, Figure S5), the protein expression of NOTCH-1 and NOTCH-2 was down-regulated (Figure 4C) whereas no

significant change in their mRNA levels was observed (Figure S5). As expected, over-expression of the MRE-containing fragment of *LncND* (1–1511 bp) in SHSY5Y cells increased the protein levels of endogenous NOTCH-1 and NOTCH-2 (Figure 4D). Taken together, these observations support the role of *LncND* as a regulator of Notch signaling.

LncND Co-regulatory Networks Direct Cells toward Neuronal Differentiation

LncND appears to sequester miR-143-3p to regulate NOTCH-1 and -2. *LncND* expression in H9 cells is correlated to *NOTCH-1* and *NOTCH-2* expression during neuronal differentiation (Figure 5A, left panel). Both increased during early stages of differentiation (day 5), but decreased at day 10 of differentiation and further decreased in neurons (Figure 5A). miR-143-3p had a distinct expression pattern. It rose with differentiation in neuroectoderm and remained elevated (Figure 5A, right panel). This pattern of *LncND* expression would allow the expression of NOTCH during early neuroectoderm stages despite the increase in miR-143-3p levels at this stage relative to the undifferentiated stem cells. On the other hand, release of miR-143-3p from *LncND* inhibits NOTCH in late neuroectoderm stages.

Because inhibition of Notch signaling in neuronal progenitor cells promotes neuronal differentiation (Wen et al., 2009 ; Louvi and Artavanis-Tsakonas, 2006), we investigated the role of *LncND* in neuronal differentiation by RNAseq. We took advantage of SHSY5Y cells, which can differentiate into neurons in the presence of all-trans retinoic acid (Constantinescu et al., 2007). Undifferentiated SHSY5Y cells were treated with siRNA against *LncND* or miR-143-3p mimic for three days and the cells were polyA$^+$ RNA-sequenced. Scrambled sequences for siRNA or miRNA mimic were used as negative controls. RNA-seq analysis revealed that 3,680 genes were down-regulated, whereas 3,026 genes were up-regulated in *LncND*-knock-down cells (Table S2, GEO: GSE73982). On the other hand, 2,389 genes were down-regulated and 1,551 genes were up-regulated after the overexpression of miR-143-3p mimic (Table S2). Among the down-regulated genes after *LncND* knock-down were those involved in the Notch signaling pathway (Figure 5B). Consistent with the prediction that the *LncND* knock-down and the miR-143-3p mimic should alter the transcriptome in the same direction, we observed a significant overlap and correlation among the differentially expressed (DE) genes (q-value<=5%) between these two experiments (p value < 0.0001, Chi-square test) (Figure 5C). The 1028 overlapping down-regulated genes contribute significantly to cell cycle processes according to DAVID GO analysis (Figure 5D). Similarly the top downregulated genes (>=1.5 fold) in *LncND* knock-down cells and miR-143-3p over-expressed cells contribute to cell cycle processes (Figure 5D). Interestingly, among the common set of down-regulated genes (1028 genes), ~45% had a perfect 6-mer match with the miR-143-3p seed region. To place this effect in terms of total down-regulated genes under the two conditions, ~44.6% of genes down-regulated after miR-143-3p overexpression had an MRE for miR-143-3p and ~41.7% of genes down-regulated after *LncND* knock-down had an MRE for miR-143-3p. In the non-overlapping set only ~ 24% of down-regulated genes had an MRE for miR-143-3p after miR-143-3p overexpression, but not after *LncND* knock-down and only ~28.2% genes of down-regulated genes had an MRE for miR-143-3p after *LncND* knock-down but not after miR-143-3p overexpression. Thus, in addition to the high concordance of the overlapping genes when

miR-143-3p is over-expressed and *LncND* is knocked-down, there was also a much lower discordance between the non-overlapping gene sets. The up-regulated genes in both of these experiments were enriched in the terms related to synapses and ion channels (Figure S6A), supporting the idea that miR-143-3p modulates the expression of multiple genes after knock-down of *LncND*.

LncND Promotes Differentiation of Progenitor Cells

LncND reduction directed cells toward neuronal identity with axon-like and dendrite-like processes (Figure 5E). To support the RNA-seq analysis and confirm the identity of these cells as neurons, we immuno-labeled them for Tau (MAPT) and MAP2 proteins, which are predominantly localized in the axons and dendrites of neurons, respectively (Kosik and Finch, 1987). The undifferentiated SHSY5Y cells express low levels of Tau and MAP2 protein (Figure 5E, top panel), whereas *LncND*-knock-down cells induced labeling of the neurites with Tau and MAP2 antibodies (Figure 5E, middle panel). The up-regulation of Tau protein is consistent with RNA-seq analysis in the *LncND* knock-down experiment in which significant up-regulation of *MAPT* transcript occurred (Table S2). *NOTCH-1* knock-down cells (~ 55% knock-down, Figure S6B) phenocopied *LncND* knock-down (Figure 5E, bottom panel) in SHSY5Y cells, supporting the idea that the neuronal differentiation phenotype is due to a reduction in NOTCH-1 protein after *LncND* knock-down. Also *NES* and *PAX6* (neural stem cell markers) mRNA expression was down-regulated in *LncND*- and *NOTCH-1* knock-down cells (Figures S6C and S6D). The phenotype was confirmed using a shRNA targeting another region of *LncND* transcript (Figure S6E). To determine whether this phenotype could be explained by the release of miRNAs bound to *LncND*, miR-143-3p mimic was over-expressed in SHSY5Y cells. We observed that miR-143-3p over-expression phenocopied *LncND*-knock-down by inducing cells with axon-like and dendrite-like processes (Figure 5F).

Following *LncND* knock-down, we observed a reduction in cell density (Figure 5F), consistent with premature differentiation of neural progenitor cells and decreased expression of cell cycle genes among differentially expressed transcripts (Figure 5D). To show the knockdown affected proliferation, we labeled cells with 5-bromo-2′-deoxyuridine (BrdU), a thymidine analog which is incorporated into newly synthesized DNA. SHSY5Y cells, treated either with control siRNA or *LncND* siRNA, were pulsed with BrdU and then fixed and stained for BrdU- and 7-aminoactinomycin D (7-AAD). ~35-40% cells, treated with control siRNA, were double positive for BrdU and 7-AAD. After three 3 days of siRNA treatment, reduction in *LncND* expression led to a highly significant decrease (~25%) in cell proliferation, as evident from the decrease in the percentage of double-positive cells (Figure 5G). *NOTCH-1* knock-down cells had a comparable reduction of ~22% in cell proliferation (Figure 5G).

Taken together, these findings suggest that low expression of *LncND* differentiates neural stem cells into neurons, due to the down-regulation of the Notch signaling pathway and several cell cycle-related genes and this effect is phenocopied by miR-143-3p overexpression.

Expression of *LncND* in Human Cerebral Organoids and Developing Human Cerebral Cortex

The Notch pathway is important for radial glia cell maintenance (Yoon et al., 2008; Gaiano et al., 2000; Shimojo et al., 2008). The Notch signaling effector gene *HES1* is highly specific to radial glia in the developing human neocortex, emphasizing the importance of Notch signaling in the maintenance of neural stem cell identity (Hansen et al., 2010). We, therefore, investigated whether *LncND* might regulate Notch signaling in radial glia cells (RGCs) in human cortex.

The expression of *LncND* was determined by single-cell RNAseq from three-dimensional cerebral organoids generated from human induced pluripotent stem cells (iPSCs) (Lancaster and Knoblich, 2014) (GEO: GSE74207). The cerebral organoid cultures had distinct germinal zones with $SOX2^+$ cells surrounding a neurotube-like structure (Figure S7A). The presence of radial glia cells was suggested by the immuno-localization of p-vimentin (Figure S7A). The apical localization of neural-specific N-cadherin was also observed (Figure S7B). We captured 68 single-cells on a C1 Single-Cell Auto Prep System (Fluidigm) and sequenced the RNA (Pollen et al., 2014). Out of 61 high quality cells, three expressed *LncND* (5% cells). The cells were hierarchically clustered according to the expression of the top 200 genes (see Methods). The smallest cluster containing all the *LncND* expressing cells (*LncND* cluster) was composed of 8 cells. 1534 genes were up-regulated and 454 genes down-regulated in this cluster as compared to all other cells (Figure S7C). Interestingly, the group of eight cells expressed significantly high levels of known RGC markers (*PAX6, FABP7,* and *NES*), Notch pathway genes (Feng et al., 1994; Hutton and Pevny, 2011; Kriegstein and Götz, 2003; Shibata et al., 1997; Götz et al., 1998; Lui et al., 2011) (Figure 6A, *LncND* expressing cells are indicated in purple bar) and neural progenitor genes including *BUB1, MKI67, AURKA, CCNA2, CCNB1, ASPM* and *DLGAP5* (Figure S7C, Table S3). No genes were differentially expressed between the *LncND* expressing cells and the other cells within the *LncND* cluster, suggesting that all 8 cells shared a transcriptional identity. This observation suggests that *LncND* is present in a relatively uniform population of cells representing RGCs in the human cerebral organoids.

We further investigated the expression domain of *LncND* during cortical development *in vivo* in humans by performing ISH in GW (gestational week) 17 cortical slices, corresponding to the peak upper cortical layer neurogenesis period (Workman et al., 2013). ISH with the probe specific for *LncND* indicated high expression in the ventricular zone (VZ) and inner subventricular zone (ISVZ) and a lower density of label in the outer subventricular zone (OSVZ) (Figure 6B). Only faint labeling was detected in the cortical plate (CP) (Figure 6B). In the OSVZ, *LncND* positive cells co-localized with PAX6 immuno-labeled cells suggesting that a population of cells expressing *LncND* are outer RGCs (Hansen et al., 2010; Götz et al., 1998; Fietz et al., 2010) (Figure 6C). This observation is consistent with the single-cell sequencing analysis in which the *LncND*-expressing cells belong to a cluster of $PAX6^+$ cells (Figure 6A). Taken together, these results suggest that *LncND* is predominantly expressed in radial glia cells in VZ and OSVZ.

Gain of *LncND* Function Leads to an Expansion of the Radial Glia Population in the Developing Mouse Cortex

Although *LncND* is not expressed in mouse, both miR-143-3p and the candidate target mRNAs coding for *NOTCH-1* and *NOTCH-2* are expressed. Based on the proposed mechanisms of *LncND* action elucidated through studies in cell lines, we hypothesized that overexpression of *LncND* would lead to an increase in Notch signaling, which supports the maintenance of radial glia (Gaiano et al., 2000; Shimojo et al., 2008; Yoon et al., 2008). To address this hypothesis, we overexpressed *LncND* in mouse radial glia by *in utero* electroporation at E13.5 (Figure 7A) and found that two days later (E15.5), a higher proportion of cells electroporated with the *LncND* construct expressed the radial glia marker pattern (Pax6+/Tbr2−) compared to control electroporated cells (Figure 7B–C). Furthermore, we detected a corresponding decrease in the proportion of TBR2+ intermediate progenitor cells, whose identity is antagonized by active Notch signaling (Yoon et al., 2008; Shimojo et al., 2008). Together, these findings suggests the role of *LncND* in the expansion of the pool of cortical radial glia cells *in vivo*.

Discussion

The results presented here describe a novel neurodevelopmental regulatory system mediated by a lncRNA that provides a spatially and temporally specific control element to co-regulate the developmental genes, Notch and miR-143-3p. The features of *LncND*, which support its function as a platform capable of Ago-mediated miR-143-3p binding to regulate NOTCH-1 and -2 are: (a) Functional sites are likely to be located in regions with little secondary structure. (b) Correlated expression patterns of the lncRNA and its miRNA(s). (c) Cytoplasmic localization of the lncRNA and its miRNA(s). (d) Competition with mRNA targets. (e) Presence in a RNA-induced silencing complex (RISC). (f) Derepression of target genes occur at physiological expression levels. (g) The derepressive effect is attributable to the miRNA binding sites. These features have been attributed to natural sponges (Ebert and Sharp, 2010). Despite the large number of lncRNAs, only a few may have a miRNA sponge-like function according to the above criteria. We found only 4–5 human brain-expressed lncRNAs with more than 10 MREs for at least one brain-expressed miRNA.

We assume the co-localization of *LncND* with miR-143-3p at the single cell level given that most of the NPCs derived from H9 and RGCs in VZ/OSVZ expressed *LncND* (Figure 1C and 6B). However, a definitive demonstration of this model will require visualization of *LncND* and miR-143-3p in the same cell. The 16 MREs for miR-143-3p likely confers efficient binding that does not result in degradation of *LncND* within a *LncND*/Ago2 complex. We found novel targets for miR-143-3p: *NOTCH-1* and *-2*. The expression patterns of these RNAs are consistent with *LncND* serving as a miR-143-3p reservoir early in neurogenesis when Notch expression is critical. Later in neural differentiation when NOTCH expression declines so does *LncND*, which releases miR-143-3p and, thereby, decreases Notch signaling specifically in *LncND*-expressing cells. Control mechanisms of this type can smoothen changes in downstream Notch signaling which would otherwise have multiplicative effects over noise in NOTCH levels. The knockdown of *LncND* promoted differentiation and reduced proliferation, consistent with the known function of NOTCH in

neuronal differentiation. However, because *LncND* has the potential to bind other miRNAs we cannot definitively attribute the *LncND* knock-down phenotype entirely to miR-143-3p despite the ability of the miR-143-3p mimic to phenocopy *LncND* knock-down. Nevertheless, the effects we observed of miR-143-3p are also consistent with the known effects of this miRNA in other tissues that include inhibition of proliferation (Kent et al., 2010; Chen et al., 2009; Cordes et al., 2009). These findings suggest a model in which *LncND* regulates the expression NOTCH during neuronal differentiation by sequestering miR-143-3p in neural precursors (Figure 7D).

Non-coding RNAs have been considered drivers of recent brain expansion (Geschwind & Rakic, 2013; Barry & Mattick, 2012) with ~20% of human lncRNAs restricted in their expression to recent branches along the human lineage and not detectable even in Rhesus (Washietl et al., 2014). Brain expansion during evolution correlates with increased cell diversity. For example, the outer subventricular zone (OSVZ), a germinal zone that expanded greatly in primates (Dehay et al., 2015), has distinctively high expression of miR-143-3p as well as miR-1912 and miR-4330 (Arcila et al., 2014), which also have MREs on *LncND*. This regulatory circuit appears to have emerged within the primate lineage when MREs for miR-143-3p, an ancient miRNA, evolved as an insertion within the more ancient lncRNA present at this locus. In the absence of the insertion, the lncRNA may have served as a *cis* control element over the neighboring gene, *TMEM18*, which mediates the migration of neural stem cells towards glioblastoma cells (Jurvansuu et al., 2008). *TMEM18* expression correlated positively with that of *LncND* upon the knock-down of *LncND* in SHSY5Y cells (data not shown). Of further relevance to tumor biology is the observation that *LncND* expression was high in SHSY5Y cells compared to glioblastoma (U251) cells or H9 hESCs (data not shown). This observation is consistent with the origin of neuroblastoma cells from early neural progenitor cells, whereas glioblastoma cells are derived from more downstream lineages in the adult brain when *LncND* would be expected to decline.

Progenitor cells in the OSVZ, which is thought to have contributed to cortical size and complexity in humans (Hansen et al., 2010) express HES1, a downstream target of the Notch pathway. Inhibition of the Notch signaling pathway has been shown to induce neuronal differentiation of OSVZ radial glia, suggesting that the Notch pathway is necessary for maintaining stemness of human oRG cells (Hansen et al., 2010; Shimojo et al., 2011; Fietz et al., 2010; Lui et al., 2011). In support of this hypothesis that *LncND* contributes to the maintenance of Notch signaling in human radial glia in VZ and OSVZ, single-cell RNA-Seq of cells captured from an *in vitro* cerebral organoid model of human cortical development and *in-situ* hybridization of primary tissue sample revealed *LncND* expression in radial glia cells. Molecular signatures for human oRG cells during cortical development (Pollen et al., 2015) and a database, CORTECON, that describes changes in RNA expression during cortical development from human embryonic stem cells (van de Leemput et al., 2014) reveal expression of *LncND* in radial glia cells and neural progenitor cells. Together, our findings suggest a molecular mechanism by which the emergence of *LncND* in primates and its co-evolution with a highly conserved miRNA-143-3p contributed to the expansion of radial glia in higher primates (Smart et al., 2002; Dehay et al., 2015).

EXPERIMENTAL PROCEDURES

Bioinformatic Analysis for prediction of MREs

miRBase 20 was used to extract the sequences of miRNAs and TargetScan 6.1 version was used for MREs for brain-expressed miRNAs for Figure 1A. For a less stringent analysis (using all miRNAs), PITA algorithm was used to identify perfect complementary pairing between the seed region 2–7 of mature miRNA sequences and the full-length *LncND*, *NOTCH-1* and *NOTCH-2.* Thermodynamic energy predictions were made using RNAHybrid (Rehmsmeier et al., 2004).

RNA *in-situ* Hybridization

RNAScope 2.0 Brown Assay (Advanced Cell Diagnostics) localized the expression of sense and antisense strand of *LncND* with probes to the complementary regions (~1000 bp). Cells were grown in chamber slides and processed according to the manufacturer's instructions. Hs-PPIB and DapB were used as positive and negative controls, respectively. Images were examined using upright Olympus BX51 microscope.

See the Supplemental Experimental Procedures for further details.

Supplementary Material

Refer to Web version on PubMed Central for supplementary material.

Acknowledgments

Mary Raven of the UCSB Microscopy Facility provided assistance. We thank UCSB Laboratory for Stem Cell Biology and Engineering, the Biological Nanostructures Laboratory within the UCSB and UCOP-supported California NanoSystems Institute and Elmer Guzman for help with RNA-sequencing. We thank Jiwon Jang for critically reading the manuscript and providing suggestions, David Bartel for insightful comments, John FredyCastro-Alvarez for technical assistance, Benjamin Purow for providing plasmid constructs for NOTCH and Israel Hernandez for sharing his unpublished data. This work was supported by the Dr. Miriam and Sheldon G. Adelson Medical Research Foundation (KSK) and R01 NS075998/NS/NINDS NIH (ARK).

References

Amaral PP, Mattick JS. Noncoding RNA in development. Mamm Genome. 2008; 19:454–492. [PubMed: 18839252]

Arcila ML, Betizeau M, Cambronne Xa, Guzman E, Doerflinger N, Bouhallier F, Zhou H, Wu B, Rani N, Bassett DS, et al. Novel primate miRNAs coevolved with ancient target genes in germinal zone-specific expression patterns. Neuron. 2014; 81:1255–1262. [PubMed: 24583023]

Artavanis-Tsakonas S. Notch Signaling: Cell Fate Control and Signal Integration in Development. Science (80-). 1999; 284:770–776.

Bail S, Swerdel M, Liu H, Jiao X, Goff La, Hart RP, Kiledjian M. Differential regulation of microRNA stability. RNA. 2010; 16:1032–1039. [PubMed: 20348442]

Barry G, Mattick JS. The role of regulatory RNA in cognitive evolution. Trends Cogn Sci. 2012; 16:497–503. [PubMed: 22940578]

Bartel DP. MicroRNA Target Recognition and Regulatory Functions. Cell. 2009; 136:215–233. [PubMed: 19167326]

Betel D, Koppal A, Agius P, Sander C, Leslie C. Comprehensive modeling of microRNA targets predicts functional non-conserved and non-canonical sites. Genome Biol. 2010; 11:R90. [PubMed: 20799968]

Bonaglia MC, Giorda R, Zanini S. A new patient with a terminal de novo 2p25.3 deletion of 1.9 Mb associated with early-onset of obesity, intellectual disabilities and hyperkinetic disorder. Mol Cytogenet. 2014; 7:53. [PubMed: 25126114]

Cabili MN, Trapnell C, Goff L, Koziol M, Tazon-Vega B, Regev A, Rinn JL. Integrative annotation of human large intergenic noncoding RNAs reveals global properties and specific subclasses. Genes Dev. 2011; 25:1915–1927. [PubMed: 21890647]

Cao X, Yeo G, Muotri AR, Kuwabara T, Gage FH. Noncoding Rnas in the Mammalian Central Nervous System. Annu Rev Neurosci. 2006; 29:77–103. [PubMed: 16776580]

Cesana M, Cacchiarelli D, Legnini I, Santini T, Sthandier O, Chinappi M, Tramontano A, Bozzoni I. A long noncoding RNA controls muscle differentiation by functioning as a competing endogenous RNA. Cell. 2011; 147:358–369. [PubMed: 22000014]

Chambers SM, Fasano Ca, Papapetrou EP, Tomishima M, Sadelain M, Studer L. Highly efficient neural conversion of human ES and iPS cells by dual inhibition of SMAD signaling. Nat Biotechnol. 2009; 27:275–280. [PubMed: 19252484]

Chen X, Guo X, Zhang H, Xiang Y, Chen J, Yin Y, Cai X, Wang K, Wang G, Ba Y, et al. Role of miR-143 targeting KRAS in colorectal tumorigenesis. Oncogene. 2009; 28:1385–1392. [PubMed: 19137007]

Chodroff, Ra; Goodstadt, L.; Sirey, TM.; Oliver, PL.; Davies, KE.; Green, ED.; Molnár, Z.; Ponting, CP. Long noncoding RNA genes: conservation of sequence and brain expression among diverse amniotes. Genome Biol. 2010; 11:R72. [PubMed: 20624288]

Constantinescu R, Constantinescu aT, Reichmann H, Janetzky B. Neuronal differentiation and long-term culture of the human neuroblastoma line SH-SY5Y. J Neural Transm Suppl. 2007:17–28. [PubMed: 17982873]

Cordes KR, Sheehy NT, White MP, Berry EC, Morton SU, Muth AN, Lee TH, Miano JM, Ivey KN, Srivastava D. miR-145 and miR-143 regulate smooth muscle cell fate and plasticity. Nature. 2009; 460:705–710. [PubMed: 19578358]

Dehay C, Kennedy H, Kosik KS. The Outer Subventricular Zone and Primate-Specific Cortical Complexification. Neuron. 2015; 85:683–694. [PubMed: 25695268]

Dereeper, a; Guignon, V.; Blanc, G.; Audic, S.; Buffet, S.; Chevenet, F.; Dufayard, JF.; Guindon, S.; Lefort, V.; Lescot, M., et al. Phylogeny fr: robust phylogenetic analysis for the non-specialist. Nucleic Acids Res. 2008; 36:465–469.

Derrien T, Johnson R, Bussotti G, Tanzer a, Djebali S, Tilgner H, Guernec G, Merkel a, Gonzalez D, Lagarde J, et al. The GENCODE v7 catalogue of human long non-coding RNAs : Analysis of their structure, evolution and expression. 2012:1775–1789.

Doco-Fenzy M, Leroy C, Schneider A, Petit F, Delrue MA, Andrieux J, Perrin-Sabourin L, Landais E, Aboura A, Puechberty J, et al. Early-onset obesity and paternal 2pter deletion encompassing the ACP1, TMEM18, and MYT1L genes. Eur J Hum Genet. 2014; 22:471–479. [PubMed: 24129437]

Ebert MS, Sharp Pa. Emerging roles for natural microRNA sponges. Curr Biol. 2010; 20:R858–R861. [PubMed: 20937476]

Ellwanger DC, Büttner Fa, Mewes HW, Stümpflen V. The sufficient minimal set of miRNA seed types. Bioinformatics. 2011; 27:1346–1350. [PubMed: 21441577]

Feng L, Hatten ME, Heintz N. Brain lipid-binding protein (BLBP): A novel signaling system in the developing mammalian CNS. Neuron. 1994; 12:895–908. [PubMed: 8161459]

Fietz, Sa; Kelava, I.; Vogt, J.; Wilsch-Bräuninger, M.; Stenzel, D.; Fish, JL.; Corbeil, D.; Riehn, A.; Distler, W.; Nitsch, R., et al. OSVZ progenitors of human and ferret neocortex are epithelial-like and expand by integrin signaling. Nat Neurosci. 2010; 13:690–699. [PubMed: 20436478]

Fineberg SK, Kosik KS, Davidson BL. MicroRNAs Potentiate Neural Development. Neuron. 2009; 64:303–309. [PubMed: 19914179]

Fox V, Gokhale PJ, Walsh JR, Matin M, Jones M, Andrews PW. Cell-cell signaling through NOTCH regulates human embryonic stem cell proliferation. Stem Cells. 2008; 26:715–723. [PubMed: 18055449]

Franco-Zorrilla JM, Valli A, Todesco M, Mateos I, Puga MI, Rubio-Somoza I, Leyva A, Weigel D, García JA, Paz-Ares J. Target mimicry provides a new mechanism for regulation of microRNA activity. Nat Genet. 2007; 39:1033–1037. [PubMed: 17643101]

Friedman RC, Farh KKH, Burge CB, Bartel DP. Most mammalian mRNAs are conserved targets of microRNAs. Genome Res. 2009; 19:92–105. [PubMed: 18955434]

Gaiano N, Fishell G. The role of notch in promoting glial and neural stem cell fates. Annu Rev Neurosci. 2002; 25:471–490. [PubMed: 12052917]

Gaiano N, Nye JS, Fishell G. Radial glial identity is promoted by Notch1 signaling in the murine forebrain. Neuron. 2000; 26:395–404. [PubMed: 10839358]

Geschwind DH, Rakic P. Cortical evolution: judge the brain by its cover. Neuron. 2013; 80:633–647. [PubMed: 24183016]

Götz M, Stoykova A, Gruss P. Pax6 controls radial glia differentiation in the cerebral cortex. Neuron. 1998; 21:1031–1044. [PubMed: 9856459]

Gregory RI, Chendrimada TP, Cooch N, Shiekhattar R. Human RISC couples microRNA biogenesis and posttranscriptional gene silencing. Cell. 2005; 123:631–640. [PubMed: 16271387]

Ha M, Kim VN. Regulation of microRNA biogenesis. Nat Rev Mol Cell Biol. 2014; 15:509–524. [PubMed: 25027649]

Hansen DV, Lui JH, Parker PRL, Kriegstein AR. Neurogenic radial glia in the outer subventricular zone of human neocortex. Nature. 2010; 464:554–561. [PubMed: 20154730]

Hansen TB, Jensen TI, Clausen BH, Bramsen JB, Finsen B, Damgaard CK, Kjems J. Natural RNA circles function as efficient microRNA sponges. Nature. 2013; 495:384–388. [PubMed: 23446346]

Hu W, Alvarez-Dominguez JR, Lodish HF. Regulation of mammalian cell differentiation by long non-coding RNAs. EMBO Rep. 2012; 13:971–983. [PubMed: 23070366]

Hutchinson JN, Ensminger AW, Clemson CM, Lynch CR, Lawrence JB, Chess A. A screen for nuclear transcripts identifies two linked noncoding RNAs associated with SC35 splicing domains. BMC Genomics. 2007; 8:39. [PubMed: 17270048]

Hutton SR, Pevny LH. SOX2 expression levels distinguish between neural progenitor populations of the developing dorsal telencephalon. Dev Biol. 2011; 352:40–47. [PubMed: 21256837]

Imig J, Brunschweiger A, Brümmer A, Guennewig B, Mittal N, Kishore S, Tsikrika P, Gerber AP, Zavolan M, Hall J. miR-CLIP capture of a miRNA targetome uncovers a lincRNA H19–miR-106a interaction. Nat Chem Biol. 2014; 11:107–114. [PubMed: 25531890]

Ji P, Diederichs S, Wang W, Böing S, Metzger R, Schneider PM, Tidow N, Brandt B, Buerger H, Bulk E, et al. MALAT-1, a novel noncoding RNA, and thymosin beta4 predict metastasis and survival in early-stage non-small cell lung cancer. Oncogene. 2003; 22:8031–8041. [PubMed: 12970751]

Jurvansuu J, Zhao Y, Leung DSY, Boulaire J, Yuan HY, Ahmed S, Wang S. Transmembrane protein 18 enhances the tropism of neural stem cells for glioma cells. Cancer Res. 2008; 68:4614–4622. [PubMed: 18559506]

Kallen AN, Zhou XB, Xu J, Qiao C, Ma J, Yan L, Lu L, Liu C, Yi JS, Zhang H, et al. The imprinted H19 lncRNA antagonizes let-7 microRNAs. Mol Cell. 2013; 52:101–112. [PubMed: 24055342]

Kent, Oa; Chivukula, RR.; Mullendore, M.; Wentzel, Ea; Feldmann, G.; Lee, KH.; Liu, S.; Leach, SD.; Maitra, A.; Mendell, JT. Repression of the miR-143 / 145 cluster by oncogenic Ras initiates a tumor-promoting feed-forward pathway service Repression of the miR-143 / 145 cluster by oncogenic Ras initiates a tumor-promoting feed-forward pathway. Genes Dev. 2010:2754–2759. [PubMed: 21159816]

Kent WJ, Sugnet CW, Furey TS, Roskin KM, Pringle TH, Zahler AM, Haussler D. The Human Genome Browser at UCSC The Human Genome Browser at UCSC. Genome Res. 2002:996–1006. [PubMed: 12045153]

Kertesz M, Iovino N, Unnerstall U, Gaul U, Segal E. The role of site accessibility in microRNA target recognition. Nat Genet. 2007; 39:1278–1284. [PubMed: 17893677]

Kosik KS, Finch Ea. MAP2 and tau segregate into dendritic and axonal domains after the elaboration of morphologically distinct neurites: an immunocytochemical study of cultured rat cerebrum. J Neurosci. 1987; 7:3142–3153. [PubMed: 2444675]

Kriegstein AR, Götz M. Radial glia diversity: A matter of cell fate. Glia. 2003; 43:37–43. [PubMed: 12761864]

Lancaster MA, Knoblich JA. Generation of cerebral organoids from human pluripotent stem cells. Nat Protoc. 2014; 9:2329–2340. [PubMed: 25188634]

van de Leemput J, Boles NC, Kiehl TR, Corneo B, Lederman P, Menon V, Lee C, Martinez Ra, Levi BP, Thompson CL, et al. CORTECON: A temporal transcriptome analysis of in vitro human cerebral cortex development from human embryonic stem cells. Neuron. 2014; 83:51–68. [PubMed: 24991954]

Legnini I, Morlando M, Mangiavacchi A, Fatica A, Bozzoni I. A Feedforward Regulatory Loop between HuR and the Long Noncoding RNA linc-MD1 Controls Early Phases of Myogenesis. Mol Cell. 2014; 53:506–514. [PubMed: 24440503]

Lewis BP, Burge CB, Bartel DP. Conserved seed pairing, often flanked by adenosines, indicates that thousands of human genes are microRNA targets. Cell. 2005; 120:15–20. [PubMed: 15652477]

Liang Y, Ridzon D, Wong L, Chen C. Characterization of microRNA expression profiles in normal human tissues. BMC Genomics. 2007; 8:166. [PubMed: 17565689]

Louvi A, Artavanis-Tsakonas S. Notch signalling in vertebrate neural development. Nat Rev Neurosci. 2006; 7:93–102. [PubMed: 16429119]

Lui JH, Hansen DV, Kriegstein AR. Development and evolution of the human neocortex. Cell. 2011; 146:18–36. [PubMed: 21729779]

Mclean CY, Reno PL, Pollen Aa, Bassan AI, Capellini TD, Guenther C, Indjeian VB, Lim X, Menke DB, Schaar BT, et al. Human-specific loss of regulatory DNA and the evolution of human-specific traits. Nature. 2003; 1:1–42.

Meister G, Landthaler M, Patkaniowska A, Dorsett Y, Teng G, Tuschl T. Human Argonaute2 mediates RNA cleavage targeted by miRNAs and siRNAs. Mol Cell. 2004; 15:185–197. [PubMed: 15260970]

Memczak S, Jens M, Elefsinioti A, Torti F, Krueger J, Rybak A, Maier L, Mackowiak SD, Gregersen LH, Munschauer M, et al. Circular RNAs are a large class of animal RNAs with regulatory potency. Nature. 2013; 495:333–338. [PubMed: 23446348]

Mercer T, Mercer T, Dinger M, Dinger M, Sunkin S, Sunkin S, Mehler M, Mehler M, Mattick J, Mattick J. Specific expression of long noncoding RNAs in the mouse brain. Proc Natl Acad Sci U S A. 2008; 105:716–721. [PubMed: 18184812]

Pollard KS, Salama SR, King B, Kern AD, Dreszer T, Katzman S, Siepel A, Pedersen JS, Bejerano G, Baertsch R, et al. Forces shaping the fastest evolving regions in the human genome. PLoS Genet. 2006; 2:1599–1611.

Pollen, Aa; Nowakowski, TJ.; Shuga, J.; Wang, X.; Leyrat, Aa; Lui, JH.; Li, N.; Szpankowski, L.; Fowler, B.; Chen, P., et al. Low-coverage single-cell mRNA sequencing reveals cellular heterogeneity and activated signaling pathways in developing cerebral cortex. Nat Biotechnol. 2014

Pollen AA, Nowakowski TJ, Chen J, Retallack H, Sandoval-Espinosa C, Nicholas CR, Shuga J, Liu SJ, Oldham MC, Diaz A, et al. Molecular Identity of Human Outer Radial Glia during Cortical Development. Cell. 2015; 163:55–67. [PubMed: 26406371]

Qureshi, Ia; Mattick, JS.; Mehler, MF. Long non-coding RNAs in nervous system function and disease. Brain Res. 2010; 1338:20–35. [PubMed: 20380817]

Rehmsmeier M, Steffen P, Höchsmann M, Giegerich R, Ho M. Fast and effective prediction of microRNA / target duplexes. 2004 Spring;:1507–1517.

Rio M, Royer G, Gobin S, de Blois M, Ozilou C, Bernheim a, Nizon M, Munnich a, Bonnefont JP, Romana S, et al. Monozygotic twins discordant for submicroscopic chromosomal anomalies in 2p25.3 region detected by array CGH. Clin Genet. 2013; 84:31–36. [PubMed: 23061379]

Shibata T, Yamada K, Watanabe M, Ikenaka K, Wada K, Tanaka K, Inoue Y. Glutamate transporter GLAST is expressed in the radial glia-astrocyte lineage of developing mouse spinal cord. J Neurosci. 1997; 17:9212–9219. [PubMed: 9364068]

Shimojo H, Ohtsuka T, Kageyama R. Oscillations in notch signaling regulate maintenance of neural progenitors. Neuron. 2008; 58:52–64. [PubMed: 18400163]

Shimojo H, Ohtsuka T, Kageyama R. Dynamic expression of notch signaling genes in neural stem/progenitor cells. Front Neurosci. 2011; 5:78. [PubMed: 21716644]

Smart IHM, Dehay C, Giroud P, Berland M, Kennedy H. Unique morphological features of the proliferative zones and postmitotic compartments of the neural epithelium giving rise to striate and extrastriate cortex in the monkey. Cereb Cortex. 2002; 12:37–53. [PubMed: 11734531]

Stevens SJC, van Ravenswaaij-Arts CMa, Janssen JWH, Klein Wassink-Ruiter JS, van Essen AJ, Dijkhuizen T, van Rheenen J, Heuts-Vijgen R, Stegmann APa, Smeets EEJGL, et al. MYT1L is a candidate gene for intellectual disability in patients with 2p25.3 (2pter) deletions. Am J Med Genet A. 2011; 155A:2739–2745. [PubMed: 21990140]

Tay Y, Kats L, Salmena L, Weiss D, Tan SM, Ala U, Karreth F, Poliseno L, Provero P, Di Cunto F, et al. Coding-independent regulation of the tumor suppressor PTEN by competing endogenous mRNAs. Cell. 2011; 147:344–357. [PubMed: 22000013]

Tay Y, Rinn J, Pandolfi PP. The multilayered complexity of ceRNA crosstalk and competition. Nature. 2014; 505:344–352. [PubMed: 24429633]

Ulitsky I, Bartel DP. lincRNAs: genomics, evolution, and mechanisms. Cell. 2013; 154:26–46. [PubMed: 23827673]

Wang J, Liu X, Wu H, Ni P, Gu Z, Qiao Y, Chen N, Sun F, Fan Q. CREB up-regulates long non-coding RNA, HULC expression through interaction with microRNA-372 in liver cancer. Nucleic Acids Res. 2010; 38:5366–5383. [PubMed: 20423907]

Wang Y, Xu Z, Jiang J, Xu C, Kang J, Xiao L, Wu M, Xiong J, Guo X, Liu H. Endogenous miRNA sponge lincRNA-RoR regulates Oct4, Nanog, and Sox2 in human embryonic stem cell self-renewal. Dev Cell. 2013; 25:69–80. [PubMed: 23541921]

Washietl S, Kellis M, Garber M. Evolutionary dynamics and tissue specificity of human long noncoding RNAs in six mammals. Genome Res. 2014; 24:616–628. [PubMed: 24429298]

Wen S, Li H, Liu J. Dynamic signaling for neural stem cell fate determination ND NO ST ND OS NO ST. 2009a:1–11.

Wen S, Li H, Liu J. Dynamic signaling for neural stem cell fate determination. Cell Adh Migr. 2009b; 3:107–117. [PubMed: 19262166]

Workman AD, Charvet CJ, Clancy B, Darlington RB, Finlay BL. Modeling Transformations of Neurodevelopmental Sequences across Mammalian Species. J Neurosci. 2013; 33:7368–7383. [PubMed: 23616543]

Yoon KJ, Koo BK, Im SK, Jeong HW, Ghim J, Kwon M chul, Moon JS, Miyata T, Kong YY. Mind Bomb 1-Expressing Intermediate Progenitors Generate Notch Signaling to Maintain Radial Glial Cells. Neuron. 2008; 58:519–531. [PubMed: 18498734]

Yu P, Pan G, Yu J, Thomson Ja. FGF2 sustains NANOG and switches the outcome of BMP4-induced human embryonic stem cell differentiation. Cell Stem Cell. 2011; 8:326–334. [PubMed: 21362572]

Zhang Z, Zhu Z, Watabe K, Zhang X, Bai C, Xu M, Wu F, Mo YY. Negative regulation of lncRNA GAS5 by miR-21. Cell Death Differ. 2013; 20:1558–1568. [PubMed: 23933812]

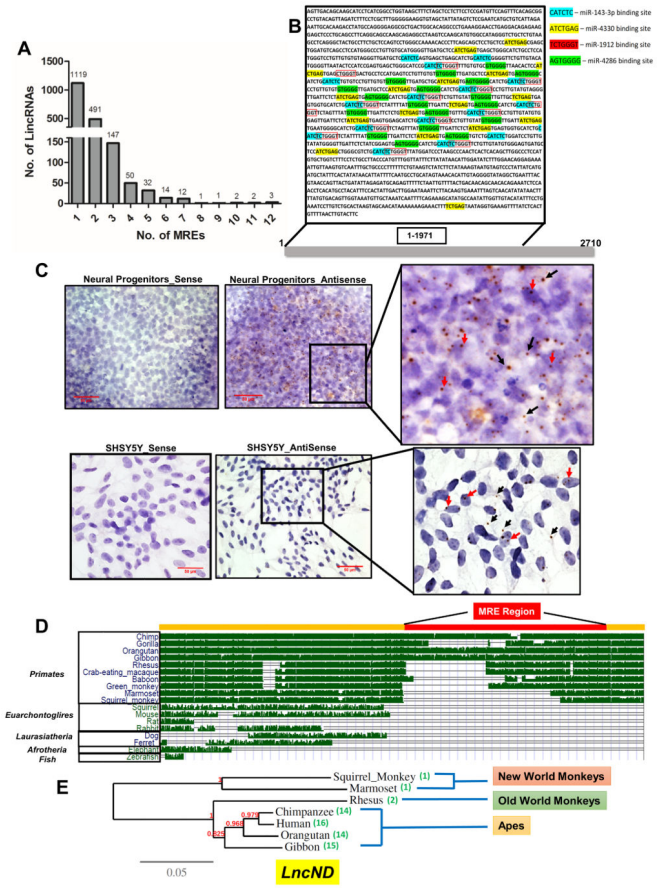

Figure 1. Identification, Characterization and Conservation of *LncND* transcript

(A) Computational prediction (using TargetScan) of all the MREs of brain-expressed miRNAs on all the brain-expressed human lncRNAs (from Human Body Map LincRNAs). The graph represents the total lncRNAs having MREs ranging from 1–12. (B) Diagrammatic representation of *LncND* transcript of 2710 bp length as annotated on UCSC Genome browser showing the MREs located in the 5′ end. Region between 1–1971 bp of *LncND* transcript is zoomed-in to show the MREs for miR-143-3p, miR-4330, miR-1912 and miR-4286. (C) *in-situ* hybridization using probes specific for either sense (left) or antisense (right) strand. Brown dots represent the positive signal for *LncND* and blue staining shows the haematoxylin nuclear stain. Black and red arrows represent the cytoplasmic and nuclear expression of *LncND*, respectively. The experiment was repeated twice with the same outcome in neural progenitor cells (top) and SHSY5Y cells (bottom). Scale: 50 μm. (D) Multiz Alignment showing the conservation of *LncND* across some representative species. Red bar represents the 5′ end of human *LncND* enriched in MREs for several miRNAs. (E) Phylogenetic relationship of *LncND* among primates. Branch lengths are based on an approximation of the standard likelihood ratio test representing the number of substitutions per site calculated by PhyML. Numbers represented in red are branch support values. The tree was created using phylogeny.fr platform. The numbers of MREs for miR-143-3p are shown in green in parenthesis.

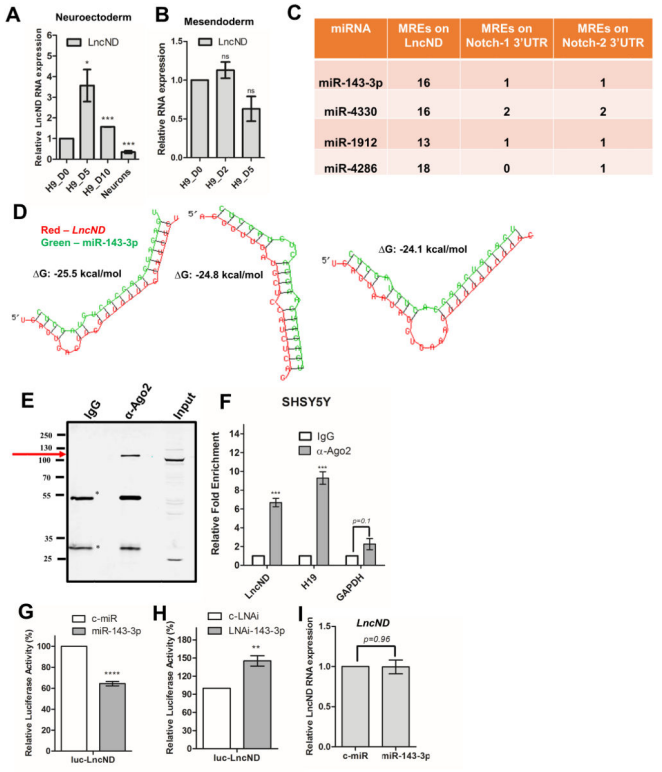

Figure 2. Expression of *LncND* and binding of miR-143-3p to *LncND* transcript

(A) H9 cells differentiated into neurons using the dual SMAD inhibition protocol. Expression of *LncND* at different time points during neuronal differentiation by RT-qPCR. (B) H9 cells differentiated into mesendoderm using BMP4 and FGF2. Expression of *LncND* during different time points of mesendoderm differentiation. (C) Table showing representative miRNAs with high number of MREs in *LncND* transcript as predicted by PITA algorithm. (D) Thermodynamic energy prediction for the association of *LncND* and miR-143-3p by RNAHybrid program. (E) RNA immunoprecipitation with either IgG or Ago2-specific antibody in SHSY5Y cells. Western blot showing Ago2 protein marked by red arrow. Asterisk (*) indicates the heavy and light chain of anti-Ago2 antibody. (F) RNA was extracted from the immunoprecipitates and analyzed by RT-qPCR. The values are represented as fold enrichment compared to the IgG control. GAPDH was used as a negative control and H19 as a positive control. (G) HEK293T cells were treated with miRNA mimics and the luciferase activity of *LncND* after 72 h was detected. Reduced luciferase activity of *LncND* was observed in the presence of the miR-143-3p mimic. (H) Increase in the luciferase activity of *LncND* after the addition of LNA inhibitor for miR-143-3p in SHSY5Y cells. Firefly luciferase activity was normalized to renilla luciferase activity. (I) The endogenous RNA expression of *LncND* after the overexpression of miR-143-3p in SHSY5Y cells by RT-qPCR. All the experiments (A-B and E-I) were performed in triplicates. Error bars represent standard deviation. *p*-values indicated were calculated by Student's t-test (unpaired). ns: $p>0.05$, *: $p\leq0.05$, **: $p\leq0.01$, ***: $p\leq0.001$, ****: $p\leq0.0001$.

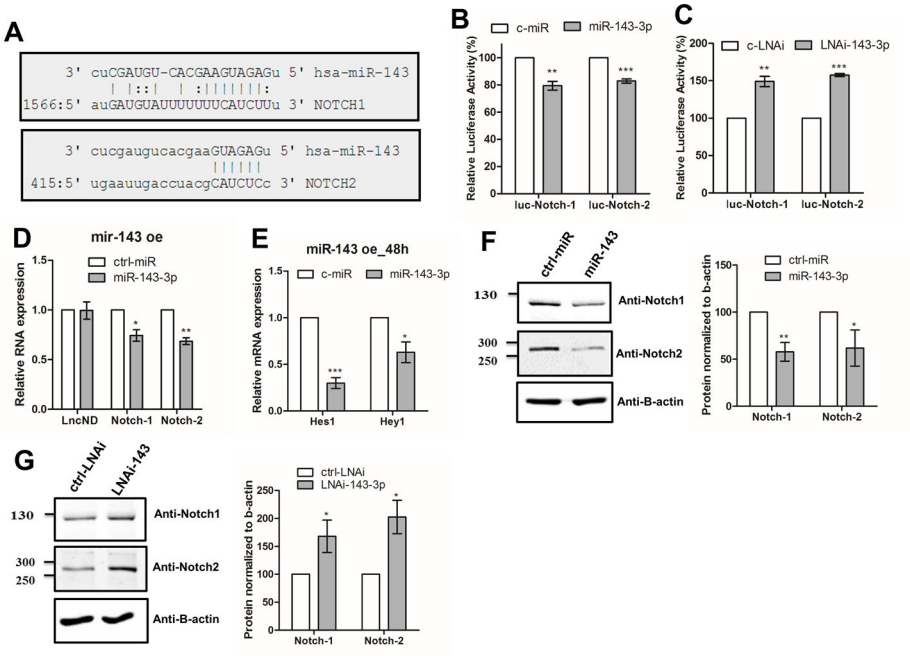

Figure 3. *NOTCH-1* and *NOTCH-2* are the targets of miR-143-3p

(A) The binding site of miR-143-3p in *NOTCH-1* and *-2* 3′UTR as predicted by PITA algorithm. (B) Validation of miRNA-binding to the 3′UTR of *NOTCH-1* and *NOTCH-2* by luciferase activity assay. Reduction in the luciferase activity demonstrated the binding of miR-143-3p to the 3′UTR of *NOTCH-1* and *NOTCH-2*. (C) Increase in the luciferase activity of *LncND* after the addition of LNA inhibitor for miR-143-3p in SHSY5Y cells. (D) Effect of miRNA overexpression on the endogenous RNA expression of *NOTCH-1*, *NOTCH-2* and *LncND* in SHSY5Y cells by RT-qPCR. (E) Down-regulation of *HES1* and *HEY1* mRNA after the overexpression of miR-143-3p in SHSY5Y cells after 48 h. (F) Immuno-blotting (left panel) and quantification (right panel) showing the reduction in the endogenous protein expression of NOTCH-1 and NOTCH-2 at 72 h following the transfection of the miR-143-3p mimic in SHSY5Y cells (G) Immuno-blotting (left panel) and quantification (right panel) showing the increase in NOTCH-1 and NOTCH-2 protein 72 h after LNA inhibition of miR-143-3p in SHSY5Y cells. qPCR results are normalized to HPRT. All experiments were performed at least three times. Error bars represent standard deviation. *p*-values indicated were calculated by Student's t-test (unpaired). ns: $p>0.05$, *: $p\leq0.05$, **: $p\leq0.01$, ***: $p\leq0.001$, ****: $p\leq0.0001$.

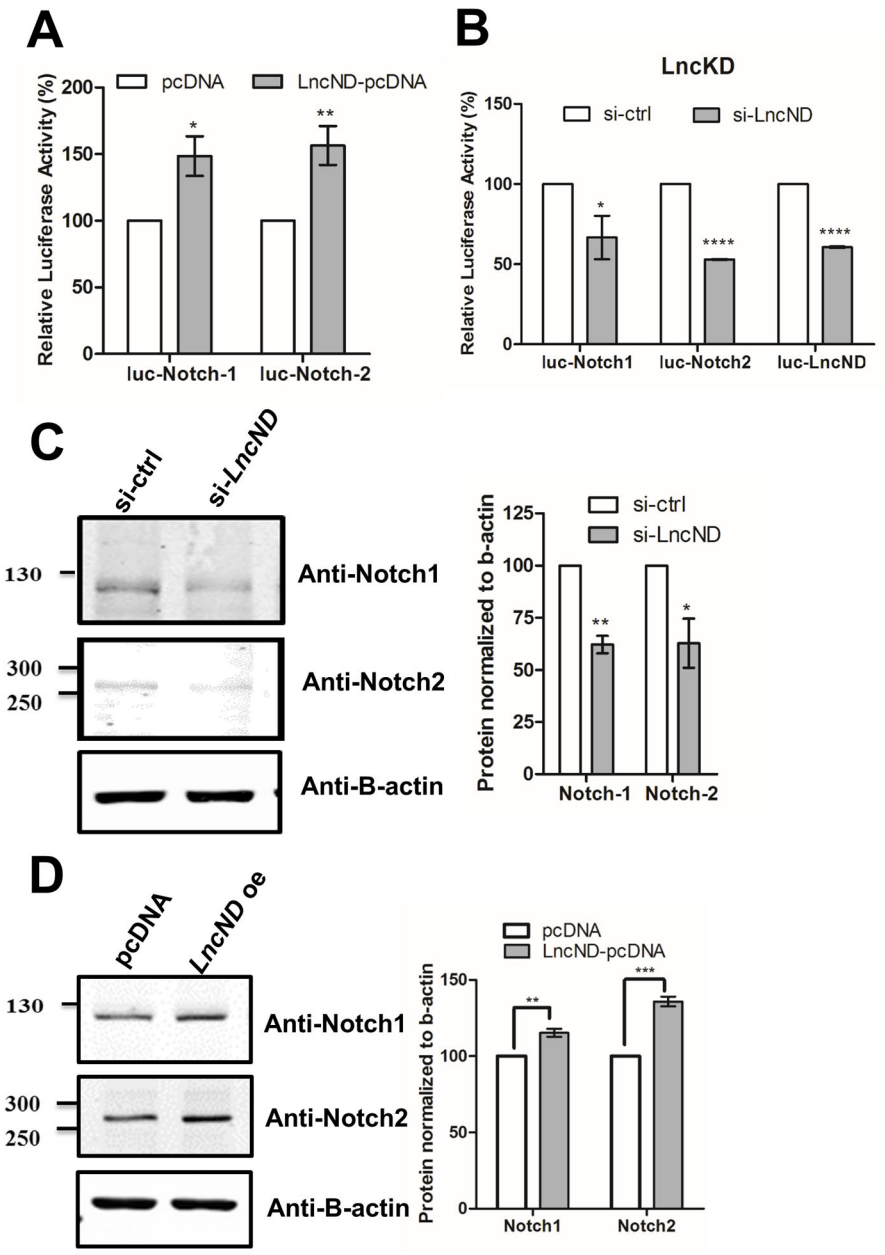

Figure 4. *LncND* act as a platform to sequester miR-143-3p

(A) The luciferase activity of *NOTCH-1* and *NOTCH-2* is up-regulated with the over-expression of *LncND* in SHSY5Y cells. (B) The luciferase activity of *NOTCH-1* and *NOTCH-2* is down-regulated with the knock-down of *LncND* in SHSY5Y cells. Firefly luciferase activity was normalized to renilla luciferase activity in all the experiments. (C) Protein expression analysis of endogenous NOTCH-1 and NOTCH-2 protein with the knock-down of *LncND* in SHSY5Y cells normalized to beta-actin. Right panel shows quantification from three replicates. (D) Overexpression of *LncND* in SHSY5Y cells increases the expression of NOTCH-1 and NOTCH-2 endogenous protein levels. Right panel shows quantification from three independent experiments. Error bars represent standard

deviation (n=3). *p*-values indicated were calculated by Student's t-test (unpaired). ns: $p>0.05$, *: $p\leq0.05$, **: $p\leq0.01$, ***: $p\leq0.001$, ****: $p\leq0.0001$.

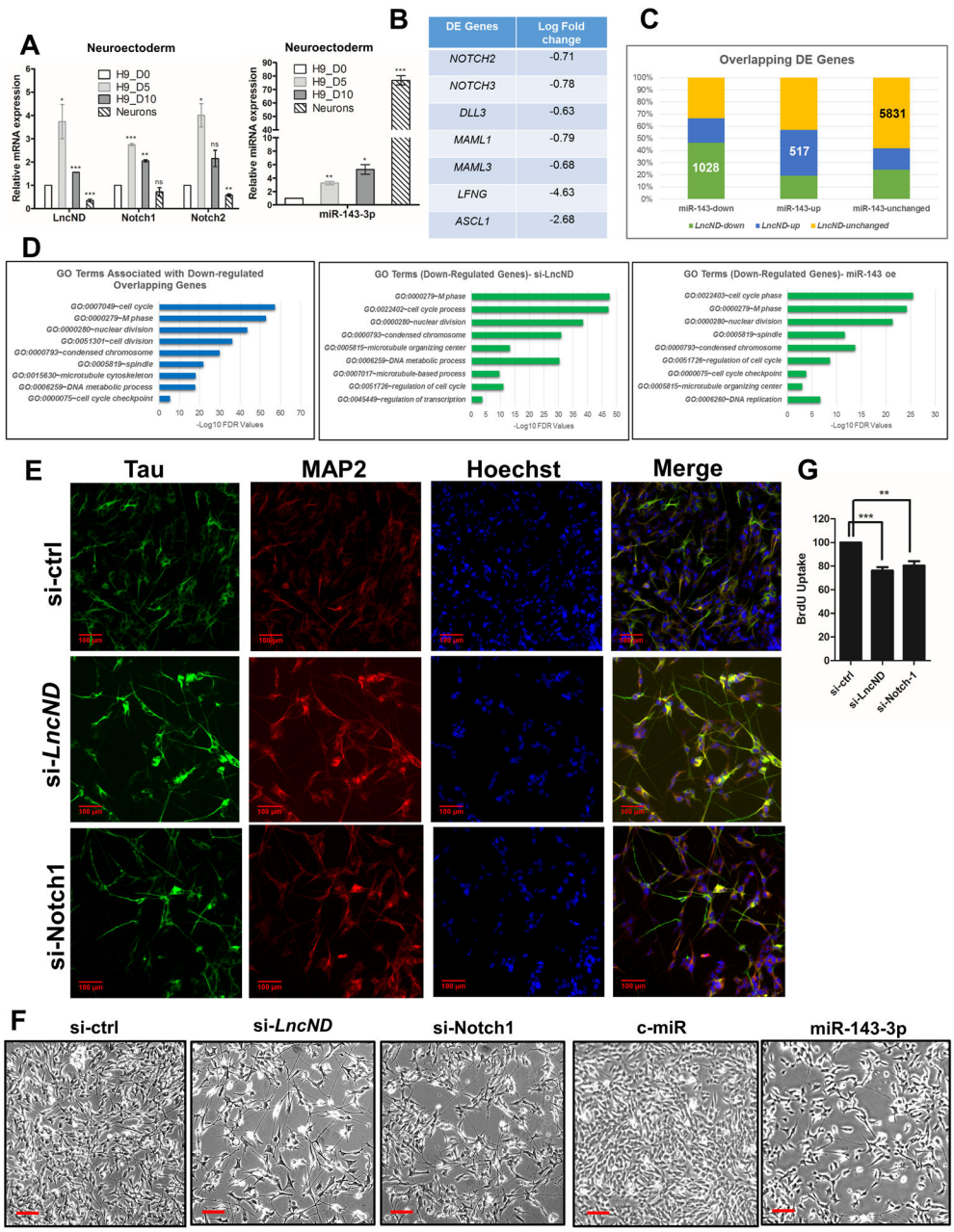

Figure 5. *LncND* knock-down leads to reduced cell proliferation and increased neuronal differentiation of SHSY5Y cells

(A) H9 cells were differentiated into neurons using dual SMAD inhibitors. RNA from cells was isolated at different time points. Left: Expression of *LncND*, *NOTCH-1* and *NOTCH-2* was analyzed by RT-qPCR at different time points during differentiation of H9 cells. Right: miRNA expression during neuronal differentiation of H9 cells was measured using Taqman probes and the values were normalized to U6. (B) Representative differentially expressed genes involved in Notch signaling as identified using Cufflinks 2.1.1 after *LncND* knock-down (n=3, q-value <= 0.05). (C) Significant correlation and overlap between genes differentially expressed or unchanged after *LncND* knock-down and miR-143-3p

overexpression (p<0.0001, Chi-square test). The numbers in the box represent the number of genes overlapping in each category. (D) Gene ontology (GO) term analysis of overlapping down-regulated genes between si-*LncND* and miR-143-3p overexpression (left), downregulated genes after *LncND* knock-down (middle) and miR-143-3p overexpression (right). (E) Immunostaining of SHSY5Y cells treated with control siRNA or siRNAs for *LncND* and *NOTCH-1*. Cells were stained for Tau (Green), MAP2 (Red) or Hoechst (Blue) for axons, dendrites and nucleus, respectively, and analyzed by fluorescent microscopy. Scale: 100 μm. (F) Bright-field image of SHSY5Y cells treated with either control siRNA, si-*LncND*, si-*NOTCH-1*, control miRNA mimic or miR-143-3p mimic. Knock-down of *LncND* and *NOTCH-1* shows neurite-like processes after 72 h of transfection. Scale: 100 μm. (G) BrdU proliferation assay. SHSY5Y cells were treated with 100 nM of either control siRNA or siRNA for *LncND* or *NOTCH-1* for 72 h. Cells stained with BrdU and 7-AAD were analyzed by flow cytometry. Knock-down of *LncND* and *NOTCH-1* significantly reduced the proliferation of SHSY5Y cells. All the experiments were performed in triplicates. Error bars represent standard deviation. p-values indicated were calculated by Student's t-test (unpaired). ***: p<0.001, **: p<0.01.

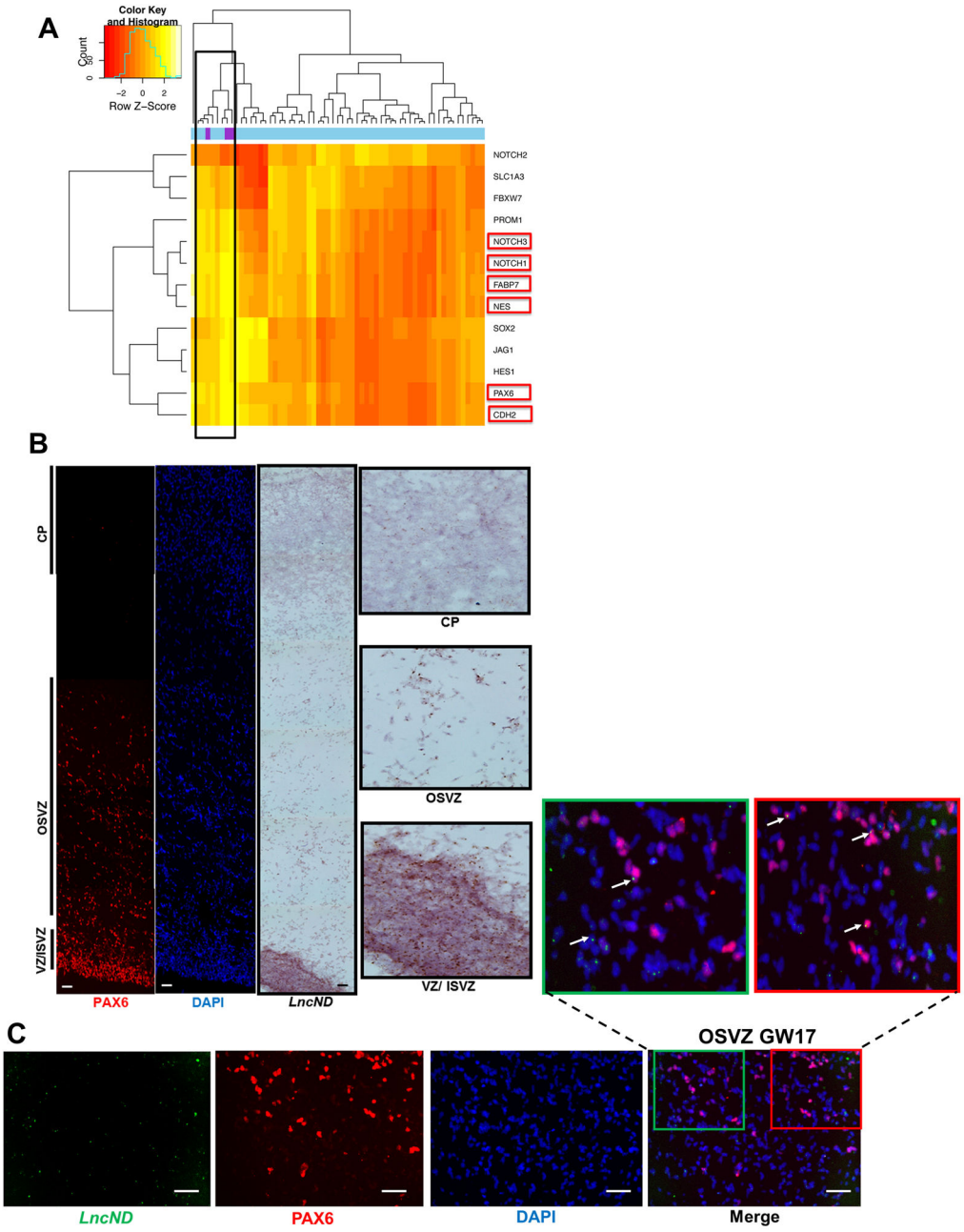

Figure 6. Expression of *LncND* in neural progenitor cells including radial glia cells in VZ and OSVZ in human neocortex

(A) Single-cell RNA-seq analysis from human cerebral organoids–Heatmap (Pearson's correlation), representing the clustering of cells based on the known radial glia cell markers. *LncND*-expressing cells are represented in purple on top of the heatmap. Genes marked in red box represents example of DE genes between *LncND*-cluster (marked in black box) and the rest of the cells. (B) Left and middle panel: GW17 primary human neocortex section demonstrating the PAX6^{+} radial glia cells and nuclear staining with DAPI. Right panel: *in-situ* hybridization with a probe specific for *LncND* showing its localization in VZ and OSVZ progenitor cells. Experiment was repeated at least two times. (C) Co-localization of *LncND*

and PAX6^{+} cells in the OSVZ representing outer radial glia cells (oRG). Red and green boxes of the merged figure are zoomed-in to show the co-localization of *LncND* and PAX6. Cells were immunostained with PAX6-specific antibody (red) after performing *in-situ* hybridization with *LncND*-specific probe (green dots). Experiment was repeated at least two times. Scale: 50μm.

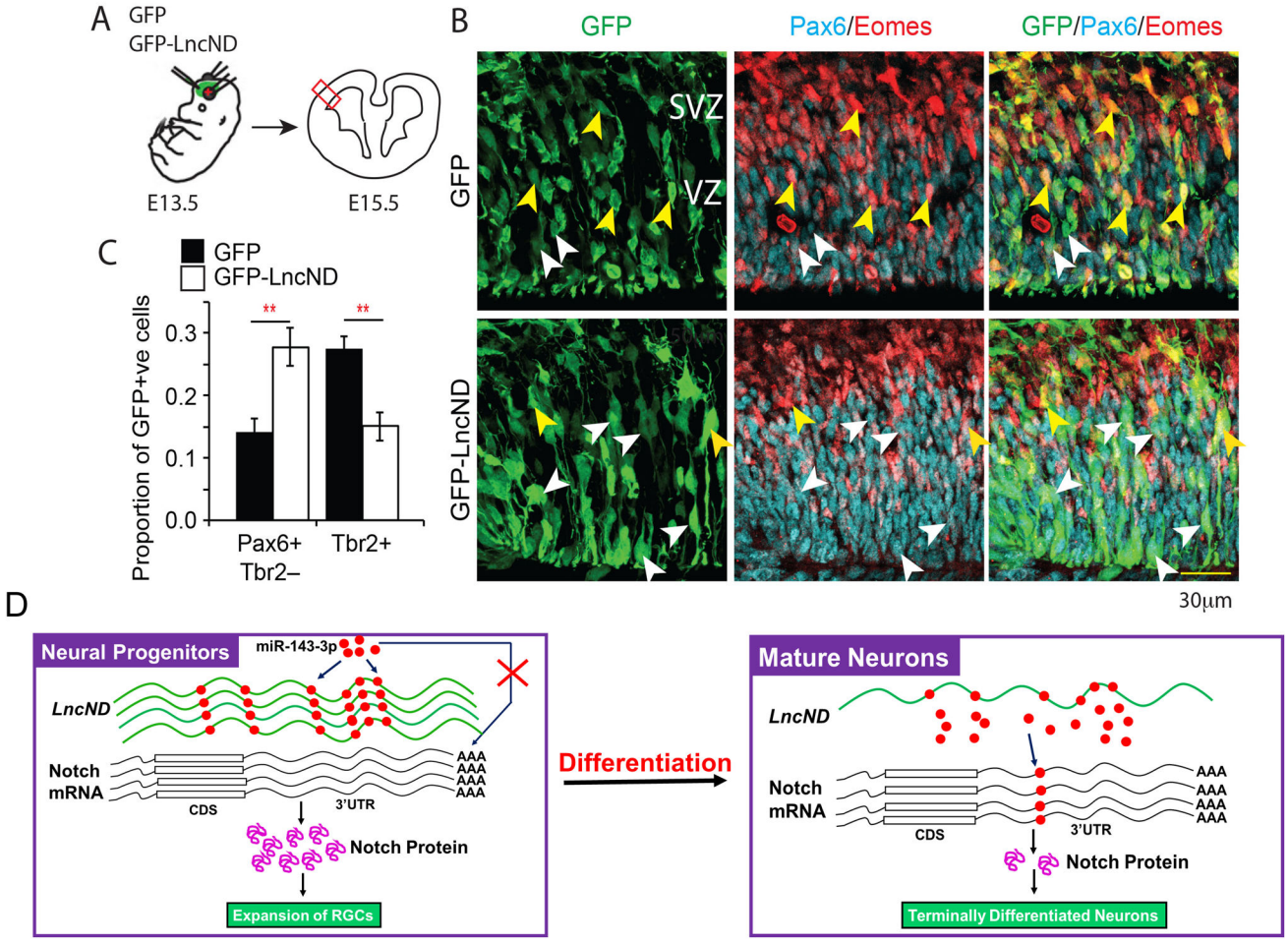

Figure 7. Gain of *LncND* function leads to an expansion of radial glia population in the developing mouse cortex

(A) Schematic representing experimental design. *LncND* was overexpressed in developing mouse E13.5 radial glia by *in utero* electroporation. Brains were harvested at E15.5 and quantification was performed in the lateral cortex (red box, see Methods). (B) Representative images of tissue sections through E15.5 mouse lateral cortex tissue sections immunostained for GFP, radial glia marker Pax6, and intermediate neuronal progenitor cell marker Tbr2. White arrowheads indicate examples of electroporated cells expressing Pax6 but not Tbr2, and yellow arrowheads indicate examples of electroporated cells expressing Tbr2. VZ-ventricular zone, SVZ-subventricular zone. (C) Bar chart represents quantification of the proportion of electroporated cells with the molecular signature of radial glia (Pax6+/Tbr2−) and intermediate progenitors (Tbr2+) in control (filled bars) and *LncND*-overexpressing conditions (open bars). ** -p<0.01, two tailed Student's t-test for n=4 biological replicates. (D) Diagrammatic representation of the molecular mechanism of *LncND* during neuronal development. In neural progenitors, *LncND* is highly expressed and sequesters miR-143-3p, thus releasing repression on the *NOTCH* mRNA leading to increased production of NOTCH proteins required for the maintenance of neural progenitors. During differentiation of neural progenitors to neurons, *LncND* expression decreases, thus releasing miR-143-3p to repress

NOTCH mRNA, supporting differentiation. RGCs: Radial glia cells, CDS: Coding DNA sequence.